Received: 2 April 2024 | Revised: 8 July 2024 | Accepted: 31 July 2024

DOI: 10.1111/ffe.14414

ORIGINAL ARTICLE

FFEMS Fatigue & Fracture of Engineering Materials & Structures WILEY

# Fatigue life improvement by shot peening for pre-fatigue tested carburized steel

**Masashi Fujino**[1] | **Toshiya Tsuji**[2] | **Koji Takahashi**[1]

[1]Yokohama National University, Yokohama, Japan

[2]Sintokogio, LTD, Toyokawa, Aichi, Japan

**Correspondence**
Koji Takahashi, Yokohama National University, 79–5, Tokiwadai, Hodogaya-ku, Yokohama-shi, 240–8501, Japan.
Email: takahashi-koji-ph@ynu.ac.jp

**Abstract**

The effect of shot peening (SP) on pre-fatigue tested carburized steel was investigated. Plane-bending fatigue tests were conducted on carburized CrMo steel that was pre-fatigue tested and treated with SP. Fatigue cracks were induced by pre-fatigue tests with a stress amplitude of $\sigma_a = 1000$ MPa, and the number of the pre-fatigue test cycles was $2.0 \times 10^4$ ($L5$ test) and $4.0 \times 10^4$ ($L15$ test). We compared the fatigue lives of the fatigue-damaged and smooth specimens without fatigue damage treated with the same SP. The fatigue life of the $L5$ tested specimens with SP was longer than that of the non-fatigue damaged smooth specimens after SP. Therefore, the fatigue cracks introduced by the $L5$ test can be rendered harmless by SP. Furthermore, near-surface material properties were evaluated and the mechanisms of rendering surface cracks harmless were investigated.

**KEYWORDS**

carburized steel, fatigue strength, remanufacturing, residual stress, shot peening

**HIGHLIGHTS**

(1) Fatigue cracks were induced by pre-fatigue tests on carburized CrMo steel.
(2) The fatigue cracks could be rendered harmless by shot peening.
(3) The mechanisms of rendering surface cracks harmless were investigated.
(4) Shot peening is expected to be utilized in remanufacturing.

## 1 | INTRODUCTION

Remanufacturing of automotive parts has attracted considerable attention in recent years.[1] Remanufacturing is rebuilding used products and components to the same quality as new ones through collection, disassembly, cleaning, and reassembly. This practice has garnered global attention as a means of achieving economic and environmental sustainability because of its resource-saving effects and superior economic efficiency compared to recycling and other methods.[2]

In the automotive parts industry, there is a high demand for remanufactured products, driven by the extensive number of vehicles in circulation.

Consequently, the remanufacturing market is being established.[2–4] Gears are among the prime candidates for remanufacturing efforts. While recycling initiatives have been undertaken for metal automotive parts like gears, these processes often entail high $CO_2$ emissions, particularly during forging and heat treatments. Remanufacturing, however, offers a pathway to mitigate these emissions by reducing the need for such energy-intensive processes. Thus, it presents a significant opportunity for $CO_2$ emissions reduction in the automotive sector. [5,6]

Gears are one of the most critical automotive parts. To improve the fatigue strength of gears, induction hardening,[7] carburizing,[8] and nitriding[9] are used. Among them, carburized steel is widely used in automotive parts such as gears. Shot peening (SP) is often applied to such parts.[8,10] SP is a mechanical surface treatment in which numerous steel shots impact the metal surface. The impact of steel shots on the metal surface at high velocities results in plastic deformation of the metal, inducing compressive residual stress, and work hardening, which leads to an improvement in the fatigue strength of the metal components. The fatigue life and fatigue limit of carburized steels were improved by SP. For example, Wang et al. reported that the fatigue life of gas-carburized CrMo steel improved by up to 650% using SP.[11] Tsuji et al. found that the fatigue limit of vacuum-carburized CrMo steel improved by up to 30% using SP.[12] Kikuchi et al. noted that the fatigue limit of gas-carburized CrMo steel could be evaluated based on surface integlities such as hardness, residual stress, and surface roughness after SP.[13]

Gears subjected to remanufacturing may have cracks on the surface of the tooth root owing to their long-term use. Because these cracks may cause gear failure, surface cracks must be rendered harmless during the remanufacturing process. It has been reported that SP can render semicircular slits harmless in spring steels (SUP9A)[14,15] and aluminum alloys.[16] The authors investigated the effect of SP on carburized CrMo steel containing a semicircular surface slit and revealed that SP can render the surface slit harmless in terms of fatigue limit.[9,17]

Several studies have been conducted to extend the fatigue life of specimens containing surface defects or pre-fatigue-damaged specimens. Saklakoglu et al. reported that SP increases the fatigue life of spring steel containing surface defects.[2,18,19] Furthermore, Ganesh et al. reported that the remaining fatigue life was improved by over 1000% by the laser peening of spring steel subjected to cyclic stress up to 50% of the fatigue life.[20] Kanazawa et al. reported that laser quenching could improve the fatigue life of friction fatigue-damaged carburized steel more than that of untreated carburized steel.[21] These studies compared the fatigue life of specimens subjected to surface treatments after the introduction of surface defects with that of smooth specimens without such surface treatments. Because peening significantly improves fatigue life, it is reasonable to use the fatigue life of surface treated smooth specimens for comparison to show that fatigue damage is rendered harmless. Therefore, previous studies have not discussed the harmless conditions of surface defects in terms of fatigue life.

In this study, plane-bending fatigue tests were performed on carburized CrMo steel specimens that had undergone fatigue damage and were subsequently treated with SP. The fatigue life (number of cycles to failure) was assessed using the Weibull distribution. We compared the fatigue life of pre-fatigued specimens and smooth specimens without fatigue damage, both treated with SP and discovered that SP effectively rendered fatigue damage harmless. Furthermore, near-surface properties such as hardness and residual stress were evaluated to discuss their influence on fatigue properties.

## 2 | EXPERIMENTS

### 2.1 | Materials and specimens

Hot-rolled round bars of CrMo steel (JIS SCM420H) with a diameter of 100 mm were used. The chemical composition of the steel is listed in Table 1. After normalizing in a vacuum, the test specimen shown in Figure 1 was machined. The specimens were fabricated such that their longitudinal direction was along the rolling direction. The specimens were then vacuum-carburized, quenched, and tempered.

### 2.2 | Pre-fatigue test and fatigue test methods

Figure 2 shows the specimen manufacturing process and experimental flow. Pre-fatigue tests were performed to induce fatigue cracks. For comparison, specimens without pre-fatigue tests were additionally prepared.

As the pre-fatigue tests, plane bending fatigue tests were carried out using a fatigue test machine (PBF-60Xa, Tokyo Koki Co. Ltd.) at a stress ratio of $R = -1$, a frequency of 20 Hz, and a stress amplitude of $\sigma_a = 1000$ MPa. The number of cycles for the pre-fatigue test was $2.0 \times 10^4$ and $4.0 \times 10^4$. The former pre-fatigue-test is referred to as the $L5$ test and the latter as the $L15$ test. The method for determining the number of test cycles for the pre-fatigue tests is described in Section 3.2.

**TABLE 1** Chemical composition of SCM420H (mass%).

| C | Si | Mn | P | S | Ni | Cr | Mo | Cu |
|---|---|---|---|---|---|---|---|---|
| 0.23 | 0.31 | 0.81 | 0.013 | 0.017 | 0.05 | 1.21 | 0.23 | 0.07 |

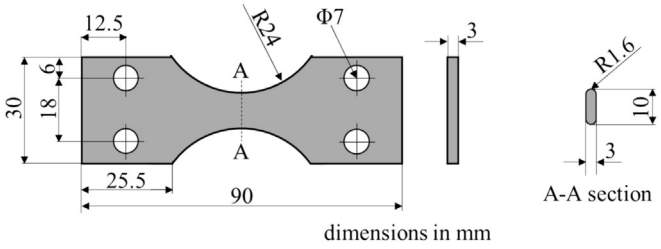


**FIGURE 1** Shapes and dimensions of the plane-bending fatigue test specimen.

Table 2 shows the SP conditions. In this study, the general SP conditions for the carburized steel were selected. This SP condition is identical to that of the previous study.[12,22] A direct air pressure-type SP equipment was used, and the shot media was a conditioned cut wire.

Fatigue tests were conducted on five types of specimens, excluding *L*15 specimens (see Figure 2). The stress amplitude $\sigma_a$ was set to 1300 MPa, and the fatigue tests were terminated until the specimen to failure. The testing machine, stress ratio, and frequency were identical to those used in the pre-fatigue test. The number of specimens $n$ used in each fatigue test was eight, and the $N_f$ values were evaluated using the Weibull distribution. However, a fatigue test was not conducted on the *L*15 specimens because they fractured at an applied stress of 1300 MPa indicating that the specimens contained fatal fatigue cracks. Optical and scanning electron microscopy (SEM) were used to observe the fractured surfaces of the specimens.

## 2.3 | Methods for measuring near-surface material properties

The surface roughness, hardness distribution, residual stress distribution, and retained austenite content of each specimen were measured.

The arithmetic mean roughness, $R_a$, and maximum height roughness, $R_y$, were measured in the longitudinal direction of the specimen.

The hardness distributions at the cross-section of the specimen were measured by using a micro-Vickers hardness tester with an indentation load of 0.98 N and a load holding time of 10 s.

An X-ray stress measuring device (μX-360s Pulstec Industrial Co., Ltd.) was used to measure distributions of residual stress and retained austenite content. The cosα method was used for the analysis. The characteristic X-ray was Cr-Kα, and the diffraction plane was α-Fe (211). Electropolishing and the measurements were repeated to obtain the residual stress and retained austenite content distributions. However, a correction calculation of the residual stress distribution was performed by considering the redistribution of residual stress owing to surface removal.[23]

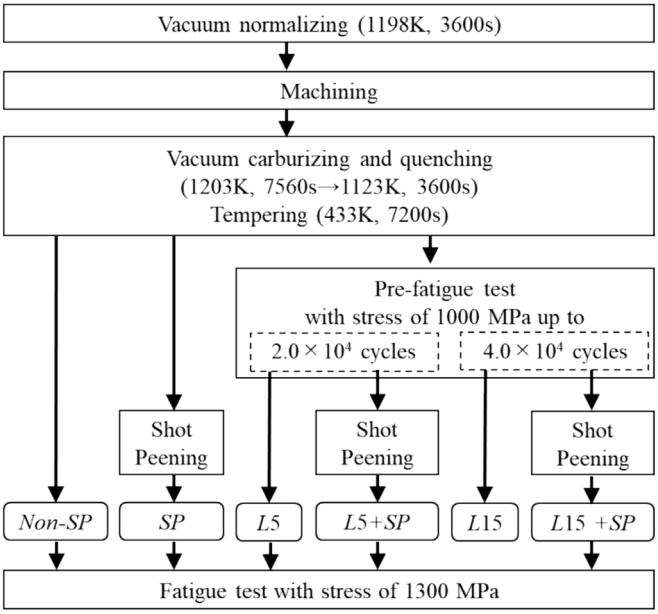


**FIGURE 2** Flow chart of preparation of specimens and fatigue tests.

# 3 | RESULT AND DISCUSSION

## 3.1 | Material property measurement results

Table 3 lists the surface roughness values of each specimen before the fatigue testing. The $R_a$ and $R_y$ values of the *SP* specimen were higher than those of the *non-SP* specimen. This was because of the dents caused by the impact of shots during the SP process.

Figure 3 shows the hardness distributions of the *non-SP* and *SP* specimens. The near-surface hardness of the *non-SP* specimen was approximately 730 HV. The effective case depth corresponding to 550 HV or higher is

**TABLE 2** Shot peening condition.

| Peening machine | Direct pressure peening |
|---|---|
| Shot media | Steel conditioned cut wire |
| Hardness of shot media (HV) | 700 |
| Diameter of shot media (mm) | 0.6 |
| Pressure (MPa) | 0.3 |
| Coverage (%) | 300 |
| Arc height (mmA) | 0.521 |

**TABLE 3** Surface roughness.

| | $R_a$ (μm) | $R_y$ (μm) |
|---|---|---|
| *Non-SP* | 0.22 | 2.71 |
| *SP* | 0.52 | 3.70 |

Abbreviation: SP, shot peening.

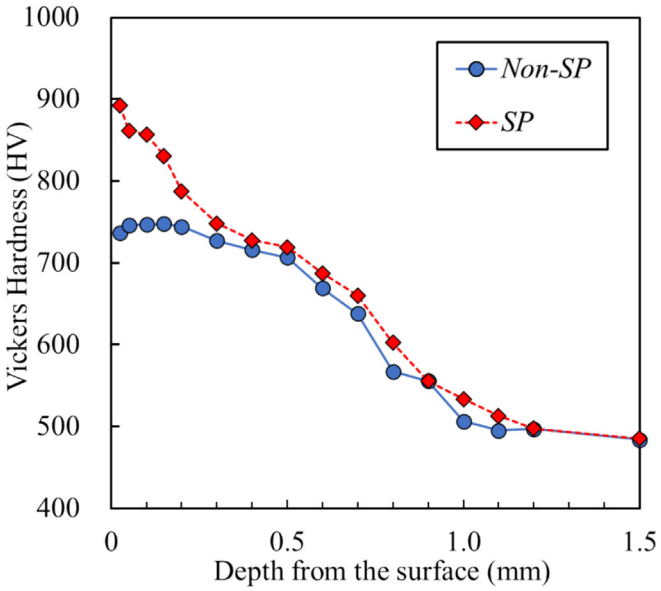


**FIGURE 3** Hardness distributions. [Colour figure can be viewed at wileyonlinelibrary.com]

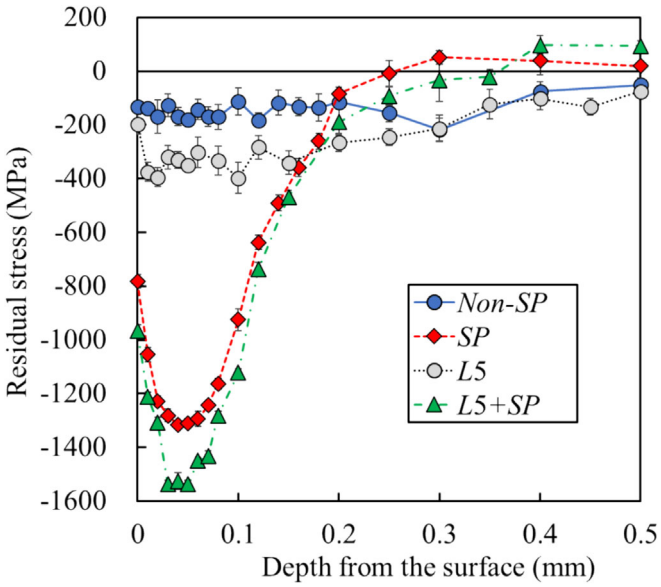


**FIGURE 4** Residual stress distributions. [Colour figure can be viewed at wileyonlinelibrary.com]

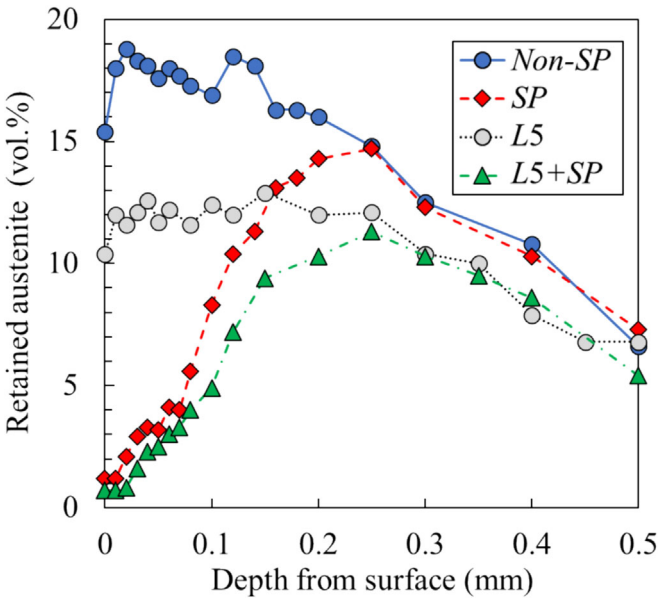


**FIGURE 5** Distribution of retained austenite. [Colour figure can be viewed at wileyonlinelibrary.com]

approximately 0.9 mm. The hardness of the *SP* specimen increased by more than 150 HV near the surface compared with that of the *Non-SP* specimen, and the hardness increased extended to a depth of 0.3 mm.

Figure 4 shows the residual stress distribution for each specimen. The compressive residual stress near the surface of the *non-SP* specimen was approximately 130 MPa. In contrast, the *SP* specimen introduced a compressive residual stress of up to 1300 MPa at a depth of approximately 0.05 mm. The crossing point where the residual stress changed from compression to tension was approximately 0.25 mm.

Figure 5 shows the distribution of the retained austenite content in each specimen. The maximum amount of retained austenite in the *non-SP* specimen is 18.8 vol. % at a depth of 0.02 mm and decreased with increasing depth. However, the amount of retained austenite in the *SP* specimen was significantly reduced compared to

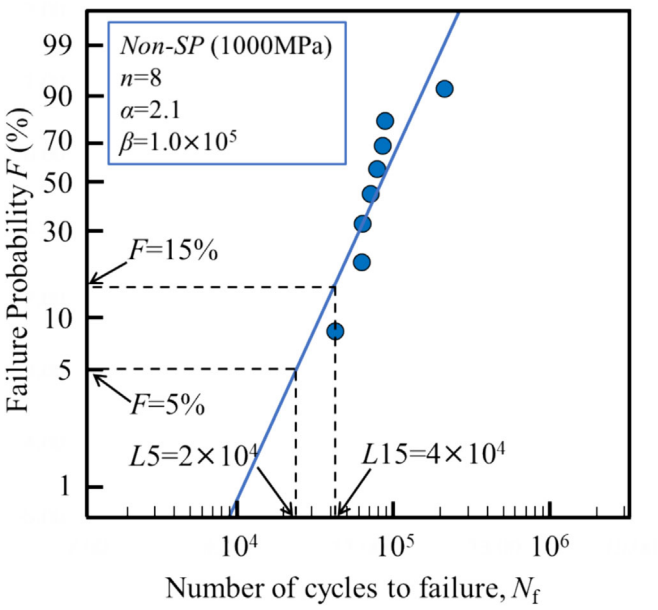


**FIGURE 6** Weibull distribution of $N_f$ of non-SP on 1000 MPa. SP, shot peening. [Colour figure can be viewed at wileyonlinelibrary.com]

that in the *non-SP* specimen in the region from the surface to a depth of 0.25 mm.

The retained austenite in carburized steel transforms into martensite after the SP process, increasing the surface hardness and compressive residual stress.[24–26] These facts suggest that the increases in hardness and compressive residual stress by SP, shown in Figures 3 and 4, were caused not only by the plastic deformation induced by shot impact but also by the strain-induced martensitic transformation of the retained austenite.

## 3.2 | Fatigue test of *Non-SP* specimen at 1000 MPa

To select the number of pre-fatigue cycles, preliminary fatigue tests were conducted at $\sigma_a = 1000$ MPa for eight *non-SP* specimens. The stress amplitudes were determined from S-N diagrams obtained in the previous study.[17] The results of preliminary fatigue tests were evaluated using a two-parameter Weibull plot. Differences in fatigue lives of surface treated metals can be effectively characterized by the use of Weibull plots.[27,28] The two-parameter Weibull distribution function is given by Equation (1).

$$F = 1 - \exp\left\{-\left(\frac{N_f}{\beta}\right)^{\alpha}\right\} \quad (1)$$

where $F$ is the cumulative failure probability calculated by the median rank method, $\alpha$ is the shape parameter indicating the degree of scatter of $N_f$, and $\beta$ is the scale parameter indicating the representative value of $N_f$ ($F = 63\%$).

Figure 6 shows the Weibull distribution of $N_f$ for the *non-SP* specimens. The $\alpha$ and $\beta$ values were 2.1 and $1.0 \times 10^5$, respectively. The average value of $N_f$ was $8.8 \times 10^4$.

In the pre-fatigue test, *non-SP* specimens with sufficient fatigue damage were required. However, the specimens fractured when subjected to excessive cycles. Therefore, $L5 = 2.0 \times 10^4$ and $L15 = 4.0 \times 10^4$ were selected as the pre-fatigue cycles that correspond to $F = 5\%$ and 15%, respectively.

## 3.3 | Fatigue test results

Figure 7 shows the S-N diagrams obtained in this study. Results from previous studies were also plotted for non-SP and SP specimens.[17] SP increased fatigue strength as shown in Figure 7(A). The values of $N_f$ of the L5 specimens were lower than that of the Non-SP. The scatter of the $N_f$ for L15 + SP specimens was larger than other specimens.

To evaluate the $N_f$ of each specimen in detail, the fatigue test results at $\sigma_a$ of 1300 MPa were organized into a Weibull distribution. Figure 8 displays the Weibull distribution for each specimen. The $N_f$ values of $\alpha$ and $\beta$ for each specimen are presented in Table 4. In subsequent discussions, $\beta$ is utilized as the representative value of $N_f$. The fatigue tests revealed that some specimens fractured from the surface, while others fractured internally. In Figure 8, specimens that fractured internally are indicated by plots with horizontal lines, whereas the others fractured from the surface.

As depicted in Figure 8(A), $N_f$ for the *SP*-treated specimen is approximately 230 times higher than that of the untreated *non-SP* specimen, indicating that the compressive residual stress induced by SP significantly enhances $N_f$. Therefore, it is appropriate to use $N_f$ of the *SP*-treated specimen over that of the *non-SP* specimen when we discuss the conditions for rendering the fatigue damage harmless by SP. However, there was increased scatter in the $N_f$ values for the *SP*-treated specimen, attributed to variations in material properties such as residual stress and surface roughness post-SP. Compared to the *non-SP* specimen, the $N_f$ of the *L5* specimen was reduced due to fatigue crack initiation in the pre-fatigue test, with scatter in $N_f$ increasing due to differences in fatigue crack size among the specimens.

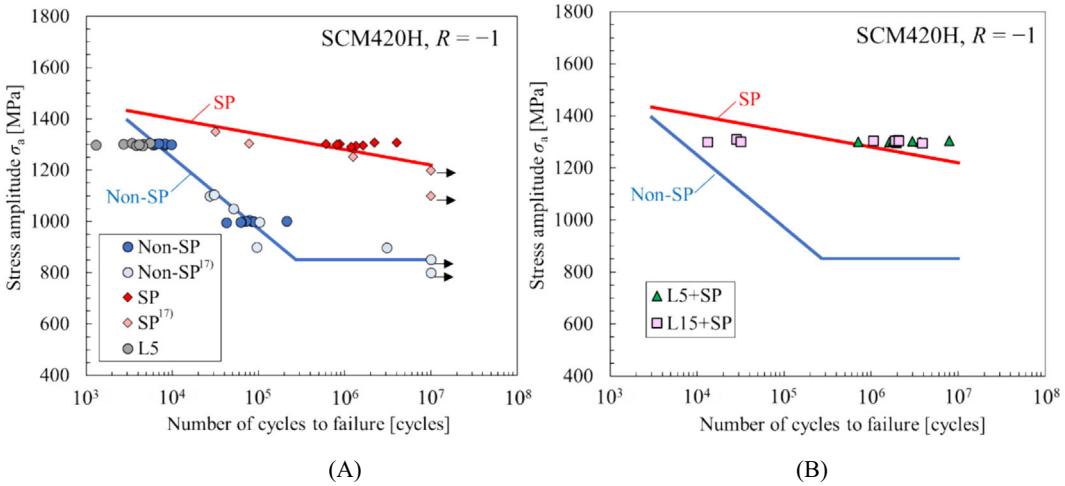


**FIGURE 7** S-N diagrams of (A) non-SP, SP, and L5 and (B) L5 + SP and L15 + SP. SP, shot peening. [Colour figure can be viewed at wileyonlinelibrary.com]

**FIGURE 8** Weibull distribution of $N_f$ for each specimen: (A) *non-SP*, *L5*, and *SP* and (b) *L5* + *SP* and *L15* + *SP*. SP, shot peening. [Colour figure can be viewed at wileyonlinelibrary.com]

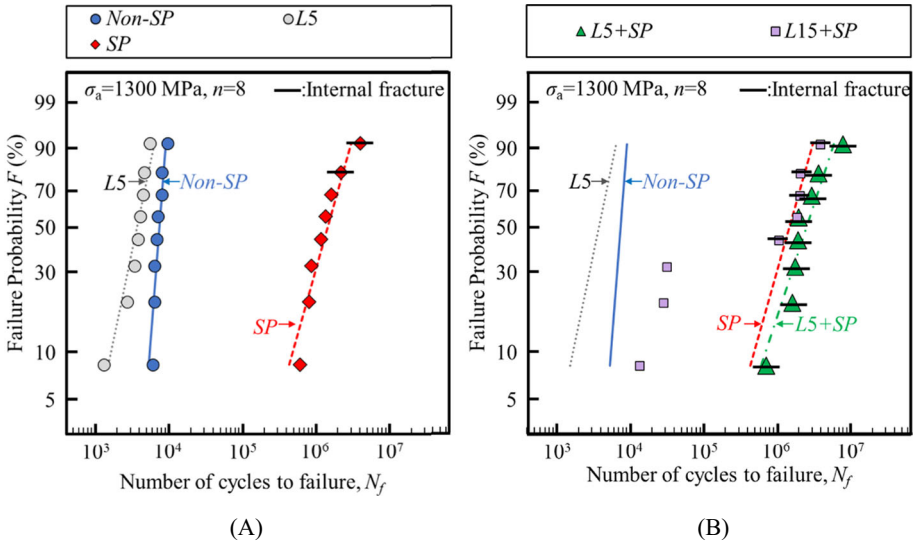


**TABLE 4** Parameters of Weibull distribution for $N_f$.

| | Non-SP | SP | *L5* | *L5* + *SP* | *L15* + *SP* |
|---|---|---|---|---|---|
| Shape parameter $\alpha$ | 6.3 | 1.7 | 2.1 | 1.5 | 0.43 |
| Scale parameter $\beta$ | $7.9 \times 10^3$ | $1.8 \times 10^6$ | $4.3 \times 10^3$ | $3.2 \times 10^6$ | $1.3 \times 10^6$ |

Abbreviation: SP, shot peening.

Figure 8(B) shows that $N_f$ of the *L5* + *SP* specimen was roughly 700 times and 1.8 times higher than those of the *L5* and *SP* specimens, respectively, demonstrating that the application of SP significantly improved $N_f$ of the *L5* specimen compared to the *SP* specimen alone.

The fatigue test results for the *L15* + *SP* specimen were categorized into two groups: five specimens with $N_f$ at the $10^6$ cycles level and three specimens with $N_f$ at the $10^4$ cycles level. Although the data plots were not linear, $\alpha$ and $\beta$ were calculated to assess the $N_f$ of the *L15* + *SP* specimen. The $\beta$ value for the *L15* + *SP* specimen was approximately 70% of that for the *SP* specimen.

## 3.4 | Fracture surface observation results

As described in the previous section, some specimens fractured from the surface, whereas others fractured from the inside. Figure 9(A),(B) show typical examples of surface and internal fractures, respectively.

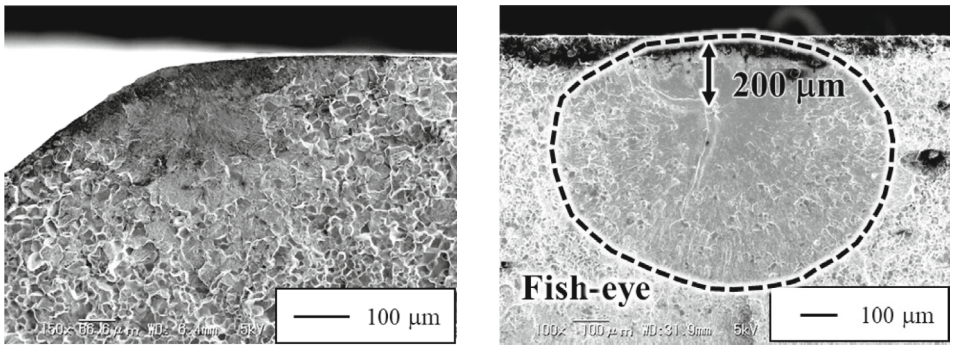


(A) (B)

**FIGURE 9** SEM observations of fatigue fracture surfaces: (A) surface fracture, *SP*, $\sigma_a = 1300$ MPa, $N_f = 6.1 \times 10^5$; (B) internal fracture, $L5 + SP$, $\sigma_a = 1300$ MPa, $N_f = 2.0 \times 10^6$. SEM, scanning electron microscopy; SP, shot peening.

The crack initiation points for all *non-SP* and *L5* specimens were located on the surface. The crack initiation points of *SP* specimens were internal for two specimens with a relatively long $N_f$ and on the surface for six specimens with a relatively short $N_f$. Even if compressive residual stress is introduced near the surface, fatigue failure may occur from dents caused by shot impact.[10,29] Because the fatigue strength depends on the size of the surface defects, specimens with harmful large dents are considered to have failed at the surface as shown in Figure 9(A). In contrast, all $L5 + SP$ specimens failed internally. In the $L15 + SP$ specimen, both surface and internal failures were observed, and the values of $N_f$ for the surface fractured specimen were much shorter than that of the internal fractured specimen. The factors affecting the fatigue behaviors of the $L5 + SP$ and $L15 + SP$ specimens are discussed in Sections 3.6 and 3.7, respectively.

Fish-eyes were observed in all internal fractured specimens, as shown in Figure 9(B). It has been reported that fatigue failure in carburized steels occurs from internal inclusions in the high-cycle fatigue range.[26,30,31] Elemental analysis by SEM–EDX confirmed the presence of MnS inclusions at the fracture origin.[9] The fracture origin was distributed at a depth of approximately 0.2 to 0.5 mm in the internal fractured specimens. Small tensile residual stresses were observed at the fracture initiation point of the specimen that failed internally.

## 3.5 | Rendering surface defects harmless in terms of fatigue life

Figure 10 presents a schematic S-N diagram comparing a smooth specimen to a specimen with surface defects, both with and without SP. This S-N diagram was drawn based on the results of Figure 7. Category (a) depicts a non-shot-peened smooth specimen; when this specimen is subjected to SP, its fatigue strength is enhanced, as shown in category (b). Conversely, when a non-shot-peened smooth specimen incurs fatigue damage, its fatigue strength diminishes, as illustrated in category (c), due to the emergence of fatal surface cracks.[32] However, if SP can neutralize the surface defects in specimen (c), an increase in fatigue strength is observed, transitioning from (c) to (d), and it is anticipated to match the fatigue strength depicted in category (b).

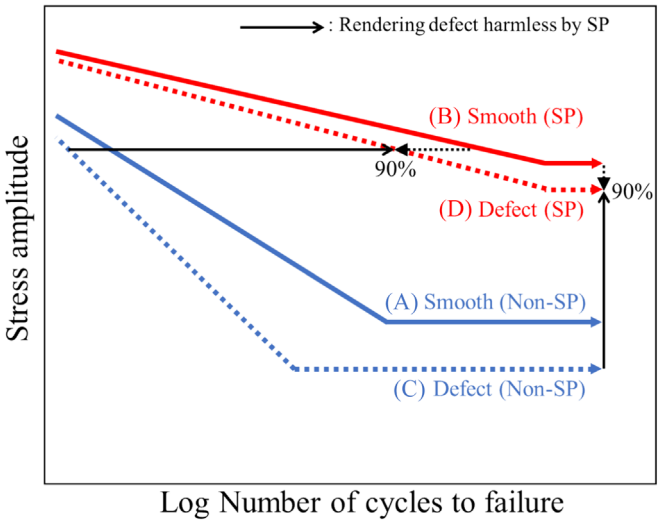


**FIGURE 10** Concept of rendering defects harmless by SP in S-N curves. SP, shot peening. [Colour figure can be viewed at wileyonlinelibrary.com]

This study defines the harmless condition for fatigue damage as the instance where the $\beta$ (the representative value of $N_f$) of a shot-peened specimen post-fatigue loading improves to exceed 90% of that of a solely SP specimen, based on precedents from previous studies.[33] Table 4 indicates that the $\beta$ of the $L5 + SP$ specimen was approximately 180% of that of the *SP* specimen, suggesting that the SP rendered the fatigue cracks from the *L5* test harmless, meeting the criteria for rendering fatigue damage harmless.

Consequently, all $L5 + SP$ specimens fractured from an internal origin, as the SP successfully neutralized the surface-initiated fatigue cracks from the *L5* test. In

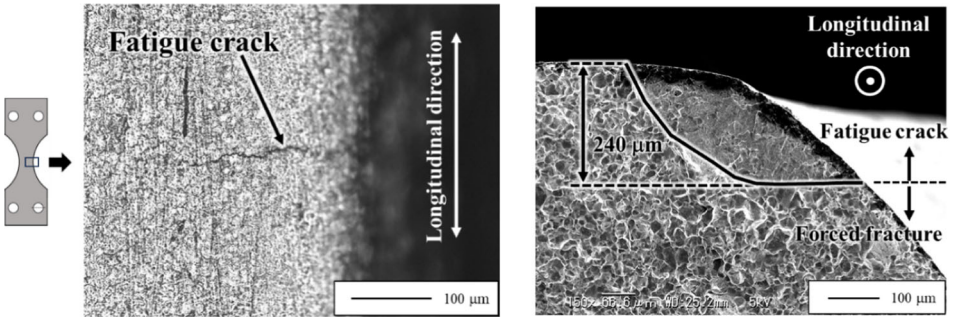


**FIGURE 11** Fatigue crack observed in the *L*15 specimen: (A) optical micrograph of fatigue crack on the surface; (B) SEM micrograph of the fracture surface. SEM, scanning electron microscopy. [Colour figure can be viewed at wileyonlinelibrary.com]

contrast, the $\beta$ of the $L15 + SP$ specimen was approximately 70% of that of the *SP* specimen, indicating that the SP was not sufficient to neutralize the fatal fatigue cracks caused by the *L*15 test.

These results show that SP can significantly improve the fatigue life of steels with cracks below a certain size. Therefore, SP is expected to be utilized in remanufacturing. It is important to apply appropriate non-destructive testing methods that can accurately assess crack dimensions.

### 3.6 | Factors increasing the fatigue life of $L5 + SP$ specimen

As mentioned in Section 3.3, the fatigue life of the $L5 + SP$ specimen was longer than that of the *SP* specimen, even though the *L*5 specimen was fatigue-damaged in the *L*5 test. To investigate this, the residual stress and retained austenite were measured for the *L*5 and $L5 + SP$ specimens.

As shown in Figure 4, the compressive residual stress in the *L*5 specimen was larger than that in the *non-SP* specimen up to a depth of 0.3 mm. Near the surface, the compressive residual stress increased by approximately 180 MPa. In the $L5 + SP$ specimen, the maximum compressive residual stress is approximately 220 MPa higher than that of the *SP* specimen. As shown in Figure 5, the amount of retained austenite in the *L*5 specimen was lower than that in the *non-SP* specimen. It is considered that martensitic transformation of the retained austenite occurred during the *L*5 test, increasing the compressive residual stress.[34–36] Consequently, the amount of retained austenite in the $L5 + SP$ specimen was lower than that in the *SP* specimen, and its compressive residual stress value was higher than that in the *SP* specimen. This is why the fatigue life of the $L5 + SP$ specimen was longer than that of the *SP* specimen, even though the *L*5 specimen was fatigue-damaged in the *L*5 test.

### 3.7 | Factors contributing to scatter in fatigue life of $L15 + SP$ specimen

As described in Section 3.3, the $N_f$ values of some $L15 + SP$ specimens were much shorter than those of the *SP* specimens. To investigate this, the surfaces of the *L*15 specimens were observed using optical microscopy and SEM. To make the surface cracks more visible, bending stresses were applied to open them for observation. As shown in Figure 11(A), only one fatigue crack was observed near the edge of the specimen surface. The *L*15 specimen was forced to static fracturing, and the fracture surface was observed using SEM, as shown in Figure 11(B). The maximum depth of the fatigue crack was 0.24 mm.

Tsuji et al. conducted fatigue tests on the same CrMo carburized steel (JIS SCM420H) with semi-circular slits of 0.1 and 0.2 mm depth after applying the SP with the same conditions.[15] They reported that semi-circular slits with a depth of 0.1 mm or less could be rendered harmless by the effect of compressive residual stresses, but slits with a depth of 0.2 mm could not be rendered harmless.[15] Therefore, fatal fatigue cracks of sizes that could not be rendered harmless by SP were considered to exist on the surface of the $L15 + SP$ specimen with short $N_f$. However, for the $L15 + SP$ specimens with $N_f$ values equivalent to those of the *SP* specimens, the initiated surface cracks were rendered harmless by SP. Therefore, the $L15 + SP$ specimens exhibited a larger scatter in fatigue life.

## 4 | CONCLUSIONS

1. Near the surface of the shot peened carburized steel (*SP* specimen), the Vickers hardness increased by 150 HV, an increase of 21%. The maximum compressive residual stress in the *SP* specimen was approximately 1300 MPa, and the depth of the residual stress was approximately 0.25 mm. The increase in hardness and compressive residual stress can be attributed to the work hardening caused by plastic deformation

resulting from shot impact and martensitic transformation of retained austenite.

2. *L5* and *L15* specimens were prepared by performing pre-fatigue tests on *non-SP* specimens at a stress amplitude of 1000 MPa for $2.0 \times 10^4$ or $4.0 \times 10^4$ cycles, respectively. The remaining fatigue life at 1300 MPa for the *L5* specimen was lower than that of the *non-SP* specimen, whereas that of the *L5* + *SP* specimen was longer than that of the *SP* specimen. Some of the *L15* + *SP* specimens had significantly shorter fatigue lives than the *SP* specimens. Consequently, the fatigue cracks caused by the *L5* test were rendered harmless, whereas those caused by the *L15* test were not rendered harmless by SP.
3. The amount of retained austenite in the *L5* specimen was lower than that in the *non-SP* specimen, suggesting that the *L5* pre-fatigue test caused a strain-induced martensitic transformation of the retained austenite. As a result, the compressive residual stress of the *L5* + *SP* specimen increased more than that of the *SP* specimen, yielding a higher $N_f$ than that of the *SP* specimen.
4. The *L15* specimen after the pre-fatigue test had a surface crack larger than the critical defect size that could be rendered harmless by SP; thus, the $N_f$ of some *L15* + *SP* specimens was shorter than that of the SP specimen.

## DATA AVAILABILITY STATEMENT

The data that support the findings of this study are available on request from the corresponding author. The data are not publicly available due to privacy or ethical restrictions.

## NOMENCLATURE

| | |
|---|---|
| $\alpha$ | shape parameter |
| $\beta$ | scale parameter |
| $\sigma_a$ | stress amplitude |
| $F$ | cumulative failure probability |
| $n$ | number of specimens |
| $N_f$ | number of cycles to failure |
| $R$ | stress ratio |
| $R_a$ | arithmetic mean roughness |
| $R_y$ | maximum height roughness |

## ORCID

*Koji Takahashi* https://orcid.org/0000-0001-5971-0582

## REFERENCES

1. Diener DL, Tillman A-M. Scrapping steel components for recycling—isn't that good enough? Seeking improvements in automotive component end-of-life. *Resour Conserv Recycl*. 2016;110:48-60.
2. Kanazawa T, Matsumoto M, Yoshimoto M, Tahara K. Environmental impact of remanufacturing mining machinery. *Sustainability*. 2022;14(13):8118.
3. Milios L, Matsumoto M. Consumer perception of remanufactured automotive parts and policy implications for transitioning to a circular economy in Sweden. *Sustainability*. 2019;11(22):6264.
4. Matsumoto M, Chinen K, Endo H. Paving the way for sustainable remanufacturing in Southeast Asia: an analysis of auto parts markets. *J Clean Prod*. 2018;205:1029-1041.
5. Bhari B, Yano J, Sakai S-I. Comparison of end-of-life vehicle material flows for reuse, material recycling, and energy recovery between Japan and the European Union. *J Mater Cycles Waste Manag*. 2021;23(2):644-663.
6. Koide R, Murakami S, Nansai K. Prioritising low-risk and high-potential circular economy strategies for decarbonisation: a meta-analysis on consumer-oriented product-service systems. *Renew Sustain Energy Rev*. 2022;155:111858.
7. Matsui K, Eto H, Yukitake K, Misaka Y, Ando K. Increase in fatigue limit of gears by compound surface refining using vacuum carburizing, contour induction hardening and double shot peening. *JSME Int J Series A Solid Mech Mater Eng*. 2002;45(2):290-297.
8. Xiao H, Chen Q, Shao E, Wu D, Chen Z, Wang Z. The effect of shot peening on rolling contact fatigue behaviour and its crack initiation and propagation in carburized steel. *Wear*. 1991;151(1):77-86.
9. Conrado E, Gorla C, Davoli P, Boniardi M. A comparison of bending fatigue strength of carburized and nitrided gears for industrial applications. *Eng Fail Anal*. 2017;78:41-54.
10. Yan H, Zhu P, Chen Z, Zhang H, Zhang Y, Zhang Y. Determination of the optimal coverage for heavy-duty-axle gears in shot peening. *Int J Adv Manuf Technol*. 2022;118(1):365-376.
11. Wang J, Qu S, Shao H, Hu X, Guo B, Li X. Ultra-high fatigue property and fracture mechanism of modified 20CrMoH steel by gas carburizing technology combined with shot peening treatment. *Int J Fatigue*. 2022;165:107221.
12. Tsuji T, Fujino M, Takahashi K. Fatigue limit improvement and rendering surface defects harmless by shot peening for carburized steel. *Metals*. 2022;13(1):42.
13. Kikuchi S, Minamizawa K, Arakawa J, Akebono H, Takesue S, Hayakawa M. Combined effect of surface morphology and residual stress induced by fine particle and shot peening on the fatigue limit for carburized steels. *Int J Fatigue*. 2023;168:107441.
14. Takahashi K, Amano T, Ando K, Takahashi F. Improvement of fatigue limit by shot peening for high-strength steel containing a crack-like surface defect. *Int J Struct Integr*. 2011;2(3):281-292.
15. Yasuda J, Takahashi K, Okada H. Improvement of fatigue limit by shot peening for high-strength steel containing a crack-like surface defect. *Int J Struct Integr*. 2014;5(1):45-59.
16. Takahashi K, Kogishi Y, Shibuya N, Kumeno F. Effects of laser peening on the fatigue strength and defect tolerance of aluminum alloy. *Fatigue Fract Eng Mater Struct*. 2020;43(4):845-856.

17. Tsuji T, Fujino M, Takahashi K. Effect of shot peening conditions on the surface defect size rendered harmless in carburized steel. *Trans Japan Soc Spring Eng.* 2024;69:55-61.
18. Saklakoglu N, Bolouri A, Irizalp SG, Baris F, Elmas A. Effects of shot peening and artificial surface defects on fatigue properties of 50CrV4 steel. *Int J Adv Manuf Technol*. 2021;112(9–10): 2961-2970.
19. Gencalp Irizalp S, Saklakoglu N, Baris F, Kayral S. Effect of shot peening on residual stress distribution and microstructure evolution of artificially defected 50CrV4 Steel. *J Mater Eng Perform.* 2020;29(11):7607-7616.
20. Ganesh P, Sundar R, Kumar H, et al. Studies on fatigue life enhancement of pre-fatigued spring steel specimens using laser shock peening. *Mater Des*. 2014;54:734-741.
21. Kanazawa T, Hayakawa M, Vinas D, Tahara Y, Hata N, Yoshimoto M. Sustainable technology for remanufacturing of carburized steels by laser hardening. *J Mater Res Technol*. 2023; 24:39-48.
22. Tsuji T, Kobayashi Y, Masaki K. Effect of residual stress distribution on the rotating bending fatigue properties of shot peening treated carburized steel. *Trans Japan Soc Spring Eng.* 2022; 67(67):75-82.
23. Society of Automotive E, Committee SAEIaST. *Residual stress measurement by x-ray diffraction -SAE J784a: report of Iron and Steel Technical Committee*. 2nded. Society of Automotive Engineers Warrendale, Pa.; 1971.
24. Fu P, Zhan K, Jiang C. Micro-structure and surface layer properties of 18CrNiMo7-6 steel after multistep shot peening. *Mater Des.* 2013;51:309-314.
25. Kobayashi Y, Tsuji T, Ishikura R, Inoue K. Influences of mechanical properties and retained austenite content on shot-peening characteristics. *Trans Japan Soc Spring Eng*. 2012; 2012(57):9-15.
26. Wu J, Wei P, Guagliano M, Yang J, Hou S, Liu H. A study of the effect of dual shot peening on the surface integrity of carburized steel: combined experiments with dislocation density-based simulations. *Arch Civ Mech Eng*. 2024;24(2):83.
27. Zhang X, Wei P, Parker RG, Liu G, Liu H, Wu S. Study on the relation between surface integrity and contact fatigue of carburized gears. *Int J Fatigue.* 2022;165:107203.
28. Klotz T, Delbergue D, Bocher P, Lévesque M, Brochu M. Surface characteristics and fatigue behavior of shot peened Inconel 718. *Int J Fatigue.* 2018;110:10-21.
29. Zhang Y, Wang J, Wu L, et al. Surface integrity and bending fatigue behavior of aeronautic gear steel under combined carburized treatment and shot peening. *Int J Fatigue.* 2023;169: 107488.
30. Nelson DV, Long Z. Bending fatigue of carburized Steel at very long lives. *J Mater Eng Perform*. 2015;25(1):220-226.
31. Böhme SA, Vinogradov A, Biermann H, Weidner A, Schmiedel A, Henkel S. Fatigue of carburised CrNiMo steel: testing and modelling concept. *Fatigue Fract Eng Mater Struct*. 2020;44(3):788-804.
32. Murakami Y, Endo M. The reality of the concept of fatigue damage in multiple step amplitude loadings: reason for unsuccessful results of existing damage counting models. *Int J Fatigue.* 2022;154:106529.
33. Fueki R, Takahashi K. Improving the fatigue limit and rendering a defect harmless by laser peening for a high strength steel welded joint. *Opt Laser Technol*. 2021;134:106605.
34. Jeddi D, Sidhom H, Ghiglione D, Lieurade H-P. Role of the cyclic stability of retained austenite in fatigue performance of carburized 14NiCr11 steel. *J Mater Eng Perform.* 2005;14(1): 37-49.
35. Ochi T, Kozawa S, Kubota M. Crack propagation behavior and change of residual stress on the process of bending fatigue test of carburized steel. *Tetsu-to-Hagané*. 2011;97(9):486-492.
36. Hayama M, Maki Y, Kikuchi S, Komotori J. Change behavior of retained austenite and residual stress on carburized SCM420H steel during fatigue process. *ISIJ Int*. 2024;64(3):ISIJINT-2023-421.

**How to cite this article:** Fujino M, Tsuji T, Takahashi K. Fatigue life improvement by shot peening for pre-fatigue tested carburized steel. *Fatigue Fract Eng Mater Struct*. 2024;47(10): 3848-3857. doi:10.1111/ffe.14414